Temperature dependent inverse spin Hall effect in Co/Pt spintronic emitters

Matthiesen, M.; Afanasiev, D.; Hortensius, J. R.; Van Thiel, T. C.; Medapalli, R.; Fullerton, E. E.; Caviglia, A. D.

DOI
10.1063/5.0010219

Publication date
2020

Document Version
Accepted author manuscript

Published in
Applied Physics Letters

Temperature dependent inverse spin Hall effect in Co/Pt spintronic emitters

M. Matthiesen,[1, a)] D. Afanasiev,[1] J. R. Hortensius,[1] T. C. van Thiel,[1] R. Medapalli,[2, 3] E. E. Fullerton,[2] and A. D. Caviglia[1, b)]

[1)]*Kavli Institute of Nanoscience, Delft University of Technology, P.O. Box 5046, 2600 GA Delft, Netherlands*

[2)]*Center for Memory and Recording Research, University of California San Diego, La Jolla, California 92093-0401, USA*

[3)]*Department of Physics, School of Sciences, National Institute of Technology, Andhra Pradesh-534102, India*

(Dated: 22 May 2020)

In bilayers of ferromagnets and heavy metals, which form so-called spintronic emitters, the phenomena of ultrafast demagnetization and the inverse spin Hall effect (ISHE) conspire to yield remarkably efficient emission of electric pulses in the THz band. Light-induced demagnetization of the ferromagnet launches a pulse of spin current into the heavy metal, wherein it bifurcates into a radiative charge transient due to the ISHE. The influence of temperature on this combined effect should depend on both the magnetic phase diagram and the microscopic origin of spin Hall conductivity, but its exact dependence remains to be clarified. Here, we experimentally study the temperature dependence of an archetypal spintronic emitter, the Co/Pt bilayer, using electro-optic sampling of the emitted THz pulses in the time domain. The emission amplitude is attenuated with decreasing temperature, consistent with an inverse spin Hall effect in platinum of predominantly intrinsic origin.

Femtosecond laser excitation of ferromagnet/non-magnetic heavy metal bilayers yields surprisingly intense emission of THz radiation, despite their nanometer thickness.[1–3] It has been argued that this emission results from the combination of ultrafast demagnetization with the inverse spin Hall effect (ISHE). Specifically, the laser excitation induces a sub-picosecond quenching of magnetization in the ferromagnetic layer through the formation of a superdiffusive spin current j_s, arising due to a larger mobility and lifetime of hot majority spins.[4–7] In the heavy metal, hot electrons of opposite spin undergo spatial deflection in opposite directions at a mean tangent $\theta_{sH} \equiv \rho_{sH}/\rho$, called the spin Hall angle, with ρ_{sH} the spin Hall resistivity of the heavy metal and ρ its longitudinal resistivity. The heavy metal thereby acts as a spin–charge transducer, converting the injected pulsed spin current $\boldsymbol{j}_s$ into a charge current $\boldsymbol{j}_c = \theta_{sH} \boldsymbol{j}_s \times \hat{\boldsymbol{m}}$, with $\hat{\boldsymbol{m}} = \boldsymbol{M}/M$ the magnetization direction. The pulsed charge current emits an electric pulse (E_{THz}) polarized perpendicularly to the initial in-plane magnetization of the sample. Due to the short timescale of demagnetization (0.2 ps), the spectral content of the emitted pulse lies in the THz band. In terms of the spin current density, the emission amplitude reads (see Supplementary Material)

$$E_{THz}(\omega) = \left(\frac{\rho_{FM|HM}}{d \rho_{HM}} \right) \rho_{sH} j_s(\omega), \tag{1}$$

Whereas the bracketed factor (which includes the resistivity of the full bilayer of thickness d) is nearly temperature independent in a bilayer of two similar metals, the THz emission amplitude may inherit a substantial temperature dependence from the remaining two quantities: the laser-induced pulsed spin current density j_s supplied by the ferromagnet, and the spin Hall resistivity[8] $\rho_{sH} = \theta_{sH} \rho$ of the heavy metal.

The temperature dependence of ρ_{sH} (or θ_{sH}) differs depending on the microscopic origin of the ISHE. The particular dependence can be ascribed either to spin-dependent scattering events (extrinsic origin), or to a geometric correction to the electron velocity arising from spin Berry curvature (intrinsic origin).[9,10] The temperature dependence of the spin current density j_s, on the other hand, is set by the degree of demagnetization $\Delta M/M_0$ of the ferromagnet. Previous studies report that the amplitude and timescale of demagnetization may depend on temperature when the ferromagnet is in proximity to a magnetic phase transition.[11–15] In this work, we use cobalt as a spin source because of its large Curie temperature ($T_C = 1388$ K in bulk[16]), meaning that below room temperature the system is far from any magnetic transition. We show that the thermal variation in this case is not set by the spin source (Co), which exhibits temperature independent magnetization and demagnetization dynamics, but instead by the spin Hall resistivity of our chosen transduction layer (Pt).

A Co(10 nm)/Pt(3 nm) bilayer is deposited by dc magnetron sputtering at room temperature onto a glass substrate that is transparent to THz radiation. A small Ar deposition pressure (3 mTorr) leads to a low degree of interface roughness[17], and a Pt residual resistivity ($T \to 0$) of $\rho_0 = 29.4\,\mu\Omega$cm. The experimental THz time-domain emission spectroscopy setup is depicted in Fig. 1. Sub-picosecond laser pulses (central wavelength 1.2 μm, repetition rate $f_{rep} = 1$ kHz) are used to demagnetize the Co layer. The emitted pulse is collected by a parabolic mirror, focused and detected with electro-optic sampling in a 0.5 mm thick ZnTe crystal cut along the (110) crystallographic direction. Complementary measurements of the magnetization and ultrafast dynamics of demagnetization are obtained via the time-resolved Faraday effect. Electronic transport measurements are carried out on a 3 nm thick Pt

[a)]Electronic mail: m.matthiesen@tudelft.nl
[b)]Electronic mail: a.caviglia@tudelft.nl

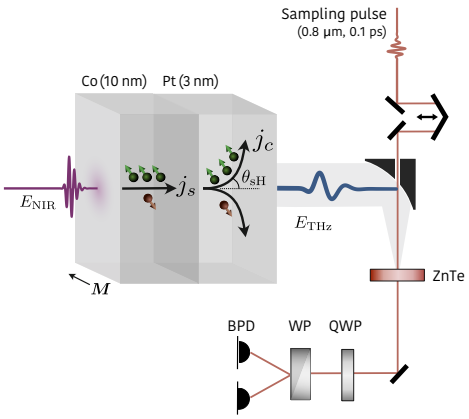

FIG. 1. Experimental scheme, consisting of two beams, one for excitation ($\lambda_0 = 1.2\,\mu$m) of the sample and one for sampling ($\lambda_0 = 0.8\,\mu$m) of the emitted THz pulse. The sampling is based on the Pockels effect in a (110)-oriented ZnTe, wherein the THz pulse modulates the polarization state of the co-propagating sampling pulse. The change in the polarization state is detected by measuring the relative intensity of the two transverse sampler field components: the components are spatially separated with a Wollaston prism (WP) and sent onto a pair of balanced photodiodes (BPD). A quarter wave plate (QWP) equalizes their intensity in the absence of a THz pulse. The spectrometer is sensitive up to about 2.7 THz (370 fs).

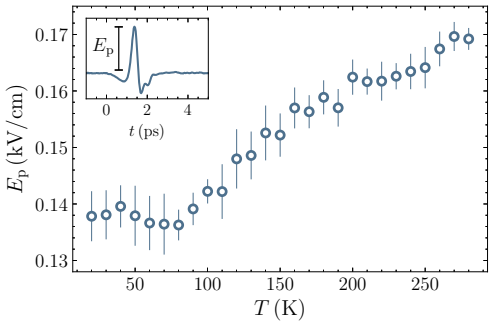

FIG. 2. Temperature (T) dependence of the peak THz emission amplitude, E_p. The inset shows an example of an emitted pulse in the time domain, measured at room temperature in a dry air environment.

film, deposited under the same conditions as the Co/Pt sample. These measurements are performed in a four-point van der Pauw geometry, sourcing a low frequency (17 Hz) 100 μA current and measuring the resulting voltage drop with a lock-in amplifier.

The peak amplitude (E_p) of the emitted pulse is measured in a temperature range of $10-280$ K, as shown in Fig. 2. The pulse shape is constant with temperature, making E_p an unambiguous measure of the emission amplitude. We observe a reduction of emission amplitude as the sample is cooled, eventually reaching a plateau at roughly 70 K. This decrease in E_p is at striking variance with the temperature behavior of THz emitters based on optical rectification, such as ZnTe and $LiNbO_3$, wherein lower temperatures reduce phonon reabsorption and enhance the emission amplitude.[18,19] The same is true of photoswitches made of InSb or GaAs, for which higher mobility at lower temperatures also contributes to enhanced THz emission.[20]

To probe whether the observed temperature dependence of E_p is due to variations in the excited spin current density j_s, we measure the temperature dependence of the magneto-optical Faraday effect. In the presence of magnetization, this causes a static rotation (θ_F) of the probe pulse polarization plane (Fig. 3a), which is proportional to the total magnetization. We observe the magnetization is independent of temperature in the $10-280$ K range. The laser-induced change in rotation ($\Delta\theta_F/\theta_F$) arising from demagnetization is presented in Fig. 3b. For the various initial sample temperatures, we extract the degree of demagnetization. We see no significant temperature dependence of the demagnetization amplitude. These observations point to ρ_{sH}, instead of j_s, as the origin of the temperature dependent THz emission amplitude.

The spin Hall resistivity $\rho_{sH} = \theta_{sH}\rho_{Pt}$ is a measure of the magnitude of the ISHE for a system with longitudinal resistivity ρ_{Pt}. It is therefore necessary to consider the temperature dependence of the Pt resistivity. For this, we deposit a 3 nm Pt film on a glass substrate separately, and measure the longitudinal resistivity as a function of temperature. We note that ρ_{sH} and ρ_{Pt} both concern the static limit ($\omega \to 0$), whereas the currents excited in the sample are transient. However, since interaction and scattering times are much shorter than the current dynamics $\omega/2\pi \approx 1$ THz, a quasi-static regime can be assumed (see Supplementary Material). The measured resistivity $\rho_{Pt}(T)$ of the bare Pt film decreases linearly from room temperature down to 30 K, below which a slight recovery occurs (Fig. 4b). Additionally, we measure the temperature dependence of the resistivity of the Co/Pt bilayer, and note that the ratio $\rho_{Co|Pt}/\rho_{Pt}$ is approximately constant to within 4% across the temperature range.

It is clear that ρ_{Pt} plays a central role in the temperature dependence of E_p, a connection which requires consideration of the microscopic origin of spin Hall resistivity, $\rho_{sH} = \sigma_{sH}\rho_{Pt}^2$. The residual resistivity of the bare Pt film is $\rho_{Pt,0} = 29.4\,\mu\Omega$cm, placing it at the boundary of two spin Hall regimes: the dominant contribution to the spin Hall resistivity arises, in one case, intrinsically from the band structure; in the other, from extrinsic skew (Mott) impurity scattering.[21] The intrinsic effect occurs due to mixing of spin states near lifted degeneracies of the spin-orbit coupled band structure. This results in a finite spin Berry curvature $\mathbf{\Omega}_{\sigma,\boldsymbol{k}}$ that modifies the semiclassical electron velocity by an amount $-\boldsymbol{k}\times\mathbf{\Omega}_{\sigma,\boldsymbol{k}}$.[22] Thus, accumulation of transverse velocity takes place during propagation rather than during scattering events. Consequently, the intrinsic spin Hall conductivity σ_{sH}^{int} does

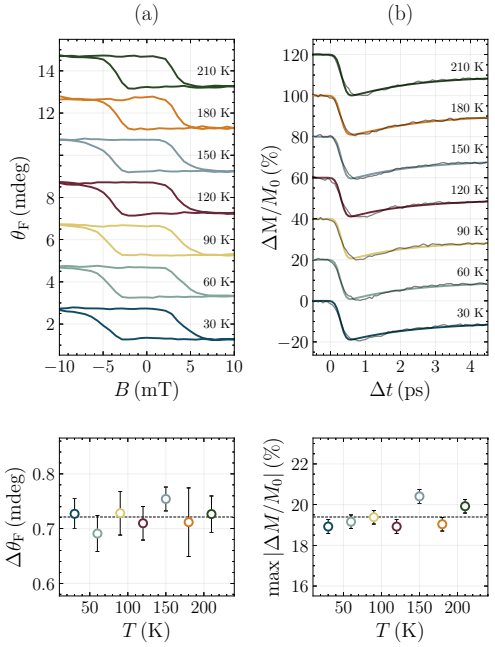

FIG. 3. (a) Hysteresis curves of the Faraday rotation θ_F are presented for various temperatures of the sample (top panel). The total rotation $\Delta\theta_F = \frac{1}{2}(\theta_F^+ - \theta_F^-)$ shown for each measured temperature (bottom panel). (b) Laser-induced dynamical changes to the magnetization, probed via the Faraday rotation, is shown for various temperatures (top panel). The peak demagnetization is extracted and plotted against T (bottom panel).

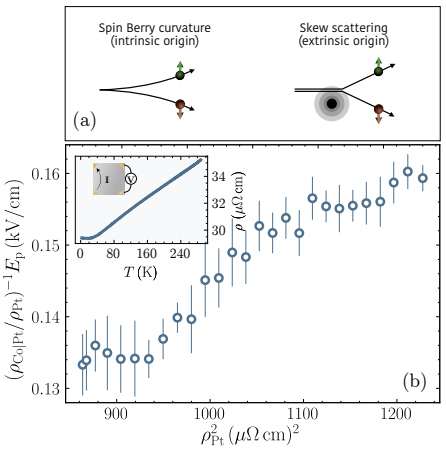

FIG. 4. (a) An illustration of the leading intrinsic and extrinsic contributions to the ISHE in Pt. (b) A measure of the spin Hall resistivity, $\rho_{sH} \propto (\rho_{Co|Pt}/\rho_{Pt})^{-1}E_p$, as a function of the squared resistivity ρ^2_{Pt}. The inset displays the temperature dependence of the resistivity ρ_{Pt}, measured in a 3 nm thick Pt film with a four-point van der Pauw scheme.

not depend on the scattering rate, so that $\rho^{int}_{SH} = \sigma^{int}_{sH}\rho^2_{Pt}$. On the other hand, skew scattering is a relativistic effect in which electrons spin-orbit coupled to an impurity experience an effective magnetic field gradient in the scattering plane. This results in a net force toward, or away, from the scattering center depending on its spin angular momentum[9] (Fig. 4a). The skew scattering contribution to the spin Hall conductivity $\sigma^{ss}_{sH} = \alpha_{ss}/\rho_{Pt,0}$ relates inversely to the residual resistivity, with α_{ss} the skew scattering angle. Furthermore, since skew scattering is impurity dependent, it is $\rho_{Pt,0}$, not ρ_{Pt}, that is the relevant resistivity. The spin Hall resistivity contribution therefore takes the form $\rho^{ss}_{sH} = \sigma^{ss}_{sH}\rho^2_{Pt,0} = \alpha_{ss}\rho_{Pt,0}$. From the above considerations, a temperature scaling of the total spin Hall resistivity has been motivated experimentally[23] and theoretically[24] to take the form

$$\rho_{sH}(T) = \alpha_{ss}\rho_{Pt,0} + \sigma^{int}_{sH}\rho^2_{Pt}(T). \quad (2)$$

In Fig. 4 we display the quantity $(\rho_{Co|Pt}/\rho_{Pt})^{-1}E_p \propto \rho_{sH}$ as a function of ρ^2_{Pt}. Comparing with Equation (2) it is clear that the observed temperature dependence follows from the presence of a substantial intrinsic contribution to the spin Hall effect. A spin Hall effect of predominantly intrinsic origin is consistently observed for Pt in experiment[8,25] and is expected from relativistic band structure calculations.[26]

While an approximately ρ^2_{Pt}–linear correlation is maintained across most of the temperature range, an unexpected amplitude recovery occurs below $T \approx 70$ K. This is at variance with Eq. (2) and warrants discussion. One possible explanation is a rise in the spin current relaxation length at low temperatures. The decay of j_s along the thickness of Pt yields a smaller effective spin current density $j^*_s \leqslant j_s$ undergoing spin–charge conversion, resulting in reduced emission. However, assuming this relaxation length is close to the spin diffusion length ($\lambda_{sd} \approx 8$ nm),[27] it is significantly longer than the thickness of our Pt film ($d_{Pt} = 3$ nm). As such, variations in λ_{sd} would have a negligible impact on E_p (see Supplementary Material). A more likely scenario is that the intrinsic spin Hall conductivity σ^{int}_{sH} has a temperature dependence, as predicted by Guo et al.[26] using first-principles relativistic band calculations for Pt. In this scenario, the Berry curvature results from the competition of two bands with contributions of opposite sign, one of which is unoccupied at $T = 0$. As the temperature is raised, the population of this band begins to reduce the net Berry curvature, thus decreasing the spin Hall conductivity. A similar temperature-dependent competition between opposing sources of emergent magnetic field has been proposed recently for ultrathin $SrRuO_3$.[28]

Using a combination of time-domain THz emission spec-

troscopy, transport measurements, and magneto-optics in a cryogenic setup, we demonstrate that the temperature response of the Co/Pt spintronic emitter is dictated by the spin Hall physics of Pt, the intrinsic origin of which leads to a proportionality between the emission amplitude and the squared resistivity of Pt. Our results highlight the relevance of cryogenic THz emission spectroscopy to the study of spin–charge conversion processes in spintronic emitters.

SUPPLEMENTARY MATERIAL

See supplementary material for a discussion on Eq. (1), the effect of spin relaxation, and the assumption of the quasistatic limit.

ACKNOWLEDGMENTS

This work was supported by The Netherlands Organisation for Scientific Research (NWO/OCW) as part of the VIDI programme and by the European Research Council under the European Unions Horizon 2020 programme/ERC Grant Agreements No. [677458], and the project Quantox of QuantERA ERA-NET Cofund in Quantum Technologies. Work at UCSD was supported by the U.S. Department of Energy, Office of Science, Office of Basic Energy Sciences under Award No. DE-SC0018237.

DATA AVAILABILITY

The data that support the findings of this study are available from the corresponding author upon reasonable request.

[1]T. Kampfrath, M. Battiato, P. Maldonado, G. Eilers, J. Nötzold, S. Mährlein, V. Zbarsky, F. Freimuth, Y. Mokrousov, S. Blügel, M. Wolf, I. Radu, P. M. Oppeneer, and M. Münzenberg, Nature Nanotechnology **8**, 256 (2013), 00179.
[2]T. Seifert, S. Jaiswal, U. Martens, J. Hannegan, L. Braun, P. Maldonado, F. Freimuth, A. Kronenberg, J. Henrizi, I. Radu, E. Beaurepaire, Y. Mokrousov, P. M. Oppeneer, M. Jourdan, G. Jakob, D. Turchinovich, L. M. Hayden, M. Wolf, M. Münzenberg, M. Kläui, and T. Kampfrath, Nature Photonics **10**, 483 (2016).
[3]T. J. Huisman, R. V. Mikhaylovskiy, J. D. Costa, F. Freimuth, E. Paz, J. Ventura, P. P. Freitas, S. Blügel, Y. Mokrousov, T. Rasing, and A. V. Kimel, Nature Nanotechnology **11**, 455 (2016).
[4]M. Battiato, K. Carva, and P. M. Oppeneer, Phys. Rev. Lett. **105**, 027203 (2010).
[5]A. Eschenlohr, M. Battiato, P. Maldonado, N. Pontius, T. Kachel, K. Holldack, R. Mitzner, A. Föhlisch, P. M. Oppeneer, and C. Stamm, Nature Materials **12**, 332 (2013).
[6]E. Turgut, C. La-o-vorakiat, J. M. Shaw, P. Grychtol, H. T. Nembach, D. Rudolf, R. Adam, M. Aeschlimann, C. M. Schneider, T. J. Silva, M. M. Murnane, H. C. Kapteyn, and S. Mathias, Phys. Rev. Lett. **110**, 197201 (2013).
[7]A. Melnikov, I. Razdolski, T. O. Wehling, E. T. Papaioannou, V. Roddatis, P. Fumagalli, O. Aktsipetrov, A. I. Lichtenstein, and U. Bovensiepen, Phys. Rev. Lett. **107**, 076601 (2011).
[8]M. Isasa, Phys. Rev. B **91**, 024402 (2015).
[9]A. Hoffmann, IEEE Transactions on Magnetics **49**, 5172 (2013).
[10]N. Nagaosa, J. Sinova, S. Onoda, A. H. MacDonald, and N. P. Ong, Rev. Mod. Phys. **82**, 1539 (2010).
[11]T. Seifert, U. Martens, S. Günther, M. a. W. Schoen, F. Radu, X. Z. Chen, I. Lucas, R. Ramos, M. H. Aguirre, P. A. Algarabel, A. Anadón, H. S. Körner, J. Walowski, C. Back, M. R. Ibarra, L. Morellón, E. Saitoh, M. Wolf, C. Song, K. Uchida, M. Münzenberg, I. Radu, and T. Kampfrath, SPIN **07**, 1740010 (2017).
[12]T. Roth, A. J. Schellekens, S. Alebrand, O. Schmitt, D. Steil, B. Koopmans, M. Cinchetti, and M. Aeschlimann, Phys. Rev. X **2**, 021006 (2012).
[13]M. Fix, R. Schneider, J. Bensmann, S. Michaelis de Vasconcellos, R. Bratschitsch, and M. Albrecht, Appl. Phys. Lett. **116**, 012402 (2020).
[14]T. J. Huisman, C. Ciccarelli, A. Tsukamoto, R. V. Mikhaylovskiy, T. Rasing, and A. V. Kimel, Appl. Phys. Lett. **110**, 072402 (2017).
[15]B. Y. Mueller and B. Rethfeld, Phys. Rev. B **90**, 144420 (2014).
[16]P. Mohn and E. P. Wohlfarth, J. Phys. F: Met. Phys. **17**, 2421 (1987).
[17]G. Li, R. Medapalli, R. V. Mikhaylovskiy, F. E. Spada, T. Rasing, E. E. Fullerton, and A. V. Kimel, Phys. Rev. Materials **3**, 084415 (2019).
[18]M. Schall and P. U. Jepsen, Appl. Phys. Lett. **77**, 2801 (2000).
[19]X. Wu, C. Zhou, W. R. Huang, F. Ahr, and F. X. Kärtner, Opt. Express, OE **23**, 29729 (2015).
[20]B. B. Hu, X.-C. Zhang, and D. H. Auston, Appl. Phys. Lett. **57**, 2629 (1990).
[21]S. Onoda, N. Sugimoto, and N. Nagaosa, Phys. Rev. B **77**, 165103 (2008).
[22]D. Xiao, M.-C. Chang, and Q. Niu, Rev. Mod. Phys. **82**, 1959 (2010).
[23]Y. Tian, L. Ye, and X. Jin, Phys. Rev. Lett. **103**, 087206 (2009).
[24]A. Shitade and N. Nagaosa, J. Phys. Soc. Jpn. **81**, 083704 (2012).
[25]L. Zhu, L. Zhu, M. Sui, D. C. Ralph, and R. A. Buhrman, Science Advances **5**, eaav8025 (2019).
[26]G. Y. Guo, S. Murakami, T.-W. Chen, and N. Nagaosa, Phys. Rev. Lett. **100**, 096401 (2008).
[27]X. Tao, Q. Liu, B. Miao, R. Yu, Z. Feng, L. Sun, B. You, J. Du, K. Chen, S. Zhang, L. Zhang, Z. Yuan, D. Wu, and H. Ding, Science Advances **4**, eaat1670 (2018).
[28]D. J. Groenendijk, C. Autieri, T. C. van Thiel, W. Brzezicki, N. Gauquelin, P. Barone, K. H. W. van den Bos, S. van Aert, J. Verbeeck, A. Filippetti, S. Picozzi, M. Cuoco, and A. D. Caviglia, arXiv:1810.05619 [cond-mat] (2018), arXiv:1810.05619 [cond-mat].